UNIFORMED SERVICES UNIVERSITY OF THE HEALTH SCIENCES
POSTGRADUATE DENTAL COLLEGE
SOUTHERN REGION OFFICE
2787 WINFIELD SCOTT ROAD, SUITE 220
JBSA FORT SAM HOUSTON, TEXAS 78234-7510
https://www.usuhs.edu/pdc

THESIS APPROVAL PAGE FOR MASTER OF SCIENCE IN ORAL BIOLOGY

Title of Thesis: "Immunohistochemical Phenotype Analysis of Cells Associated with Pulpal Mineralized Extracellular Matrix in a Porcine Endodontic Regeneration Model."

Name of Candidate: CPT (P) Joshua D. Pruden
Master of Science Degree
June 13, 2018

THESIS/MANUSCRIPT APPROVED: DATE:

[redacted]

Joseph M. Dutner, MAJ, DC
DEPARTMENT OF ENDODONTICS, FOR GORDON
Committee Chairperson

[redacted]

Stephanie J. Sidow, COL, DC
DEPARTMENT OF ENDODONTICS, FORT GORDON
Committee Member

[redacted] 23 May 2018

Dr. Douglas Dickinson
DEPARTMENT OF CLINICAL INVESTIGATION, FORT GORDON
Committee Chairperson

"The author hereby certifies that the use of any copyrighted material in the table thesis/dissertation manuscript entitled:

"Immunohistochemical Phenotype Analysis of Cells Associated with Pulpal Mineralized Extracellular Matrix in a Porcine Endodontic Regeneration Model"

is appropriately acknowledged and, beyond brief excerpts, is with the permission of the copyright owner.

[redacted]

CPT(P) Joshua Pruden
Advanced Education Program in Endodontics
Uniformed Services University
23 May 2018

Distribution Statement

Distribution A: Public Release.

The views presented here are those of the author and are not to be construed as official or reflecting the views of the Uniformed Services University of the Health Sciences, the Department of Defense or the U.S. Government.

Immunohistochemical Phenotype Analysis of Cells Associated with Pulpal Mineralized Extracellular Matrix in a Porcine Endodontic Regeneration Model

Joshua Pruden, DDS, Douglas Dickinson, PhD, Stephanie Sidow, DDS, Joseph Dutner, DMD

Abstract

Introduction: Early apical mineralization responses following regeneration therapy remain to be fully characterized, partially due to limited availability of larger animal models. The aims were to evaluate a young porcine model for the study of endodontic regenerative treatment, and to compare via immunohistochemistry the early cellular and mineralizing events occurring at the apex following therapies utilizing Biodentine™ (Septodont, Saint Maur des Fosses, France) and Pro-Root MTA™ (Dentsply Sirona, Tulsa, OK).

Methods: Immunohistochemical techniques were used to characterize cell populations and mineralized tissues in samples previously obtained from a study utilizing a young porcine model for endodontic regeneration in which mandibular first and second premolars in five pigs (3 months old) received regenerative treatment. Teeth were divided into five treatment groups: One: treated with blood clot without bioceramic; Two: treated with blood clot and MTA; Three: treated with blood clot and Biodentine; Four: treated with MTA without blood clot (positive control); and Five: no treatment (positive/negative control). Samples were harvested after a three-week healing period, fixed in formalin, evaluated radiographically, and processed for histology. Sections were stained immunohistochemically for mineralized matrix markers,

including dentin sialophosphoprotein, osteocalcin, osteopontin, cementum-attachment protein, osterix, and proliferating cell nuclear antigen.

Results: The blood clot treatment groups and MTA/Biodentine treatment groups demonstrated extensive areas of active hard tissue matrix formation on the canal walls, resembling cellular cementum-like deposition extending from the apex, with high levels of cementoblast-like cell activity.

Conclusions: A cementum-like mineralization of potential clinical benefit can occur in the apical root region following endodontic regenerative treatment. The porcine model shows promise for the study of these events.

Introduction

The pulp in an immature tooth with an open apex can become necrotic, resulting in challenges for treatment. The roots of an immature tooth are short, thin, and prone to fracture, conditions for which conventional root canal treatment is not ideal. Importantly, there is a need to allow the root to grow in both length and thickness in order to withstand normal forces of function, including mastication. Regeneration endodontics aims to both increase the length and thickness of the root (1), and has been defined as ‘‘biologically based procedures designed to replace damaged structures, including dentin and root structures, as well as cells of the pulp-dentin complex’’ (2). In principle, the damaged pulp can heal by two mechanisms: repair or regeneration. Repair is defined as ectopic tissue formation with a partial loss of function, and endodontic studies have variously reported fibrous tissue, cementum, or bone forming inside the canal (3, 4, 5, 6, 7).

The development of mineralized tissue by regeneration requires stem/progenitor cells (that can differentiate into requisite cells such as odontoblasts) to migrate, proliferate, and differentiate appropriately. These cellular processes can be promoted by the presence of appropriate concentrations of growth factors and a supporting scaffold (8). Endodontic regeneration strategies include initiating bleeding at the apex to form a blood clot within the canal, thereby providing a scaffold and source of growth factors (via platelets), and providing an environment conducive for stem cell/progenitor cells to migrate, proliferate, and differentiate, ultimately leading to mineralized tissue formation (9). Additionally, endodontic regeneration strategies include placement of bioactive materials to promote mineralized tissue formation and to protect against infection and

coronal microleakage. Mineral Trioxide Aggregate (MTA) and Biodentine™ are two bioceramic sealing materials that have been shown to be superior in providing a seal, forming hard tissue, and stimulating stem cell differentiation (10, 11, 12).

Numerous case reports and case series of endodontic regeneration treatments have been published, but many do not analyze the properties of the formed tissues; histological studies of endodontic regeneration in humans are scarce, due to the goal of retention of the tooth after successful treatment (13). Primarily, regenerative treatment outcomes have been evaluated clinically and radiographically, showing continued hard tissue formation in the canal, increasing width and length of the root (14, 15).

Animal models for endodontic regeneration employing rats, dogs, ferrets, and most recently pigs have been studied. The domestic pig (Sus scrofa) provides a large animal model for oral tissues resembling human oral tissues (16). The posterior teeth in a young pig have large multiple-rooted teeth with open apices and incomplete root development (17). Therefore, a young pig has underdeveloped teeth similar to immature human teeth. Furthermore, pigs have mandibular canine teeth that erupt continuously (17), providing additional tissues with which to compare and analyze regenerative physiological mechanisms. Overall, the porcine endodontic regenerative model could provide a useful model system to investigate the biology of the endodontic regenerative process.

Recently, a porcine model for endodontic regeneration using young animals with immature teeth was developed that shows considerable promise (18). Using this model, rapid formation of a mineralizing lining of the root canal was demonstrated using

regeneration treatment modalities and tissue analysis by histochemical staining (18). Three weeks after initiating the treatment, 5-6mm of mineralized tissue was observed on the canal walls of the pulp. However, the cellular events in this model during induced mineral formation remain to be characterized. Further, the mineralized tissue did not resemble a dentin-like matrix, nor did it closely resemble an osteoid-like matrix, but had similarities to cementum. If the mineralized tissue produced during regenerative treatment could be characterized and identified via immunohistochemical evaluation, then more light would be shed on the biological mechanisms underlying endodontic regeneration. This would provide the basis for rational approaches to the development of improved and new strategies for endodontic regeneration, leading to more predictable treatment outcomes, and likely improve the prognosis of tooth retention. Therefore, the aims of this study were to evaluate the young porcine model for the study of endodontic regenerative treatment and to compare via immunohistochemistry the early cellular and mineralizing events occurring at the apex following therapies using Biodentine™ (Septodont, Saint Maur des Fosses, France) and Pro-Root MTA™ (Dentsply Sirona, Tulsa, OK).

Materials and Methods:

Study samples obtained from an Eisenhower Army Medical Center IACUC approved study (IRBNet #: 415705-1). Investigators adhered to the policies of the Animal Welfare Act. All animal procedures were approved by the Dwight D. Eisenhower Army Medical Center Institutional Animal Care and Use Committee (IACUC), and the IACUC ethical guidelines and regulations were adhered to throughout.

Histological sections of a porcine regeneration model were obtained from a previous study (18). Five pigs (3 months old) received regenerative treatment in their second and third mandibular premolars, resulting in four teeth receiving treatment per animal (total n=20). Teeth received endodontic regenerative therapy with variations in technique. Teeth in Group One had induced bleeding (with a #20 K file) and received a glass ionomer restorative material (Fuji II LC; GC America, Alsip, IL). Teeth in Group Two underwent induced bleeding and were sealed with MTA. Teeth in Group Three also underwent induced bleeding but were sealed with Biodentine. Teeth in Group Four received a MTA coronal restoration but a blood clot was not induced. Group Five consisted of a randomly selected canine that did not receive endodontic treatment. In the previous study, samples were harvested after a three-week healing period, fixed in 10% formalin, evaluated radiographically, and processed for histology.

In the current study, histological sections underwent an immunohistochemical process for each of the selected antibody markers being tested for a positive signal. These included the mineralization markers dentin sialophosphoprotein (DSPP), osteocalcin (OCN), osteopontin (OPN), and cementum-attachment protein (CAP). The mineralization transcription factor marker was osterix (OSX), and the cell proliferation marker was proliferating cell nuclear antigen (PCNA). The staining protocol for the staining of each marker extended over three days. Day One, slides were heated at 60^0C for two hours, followed by immediate placement in fresh xylene to begin de-paraffinization overnight. Day Two, de-paraffinization was completed by placing the slides and xylene at 40^0 C, followed by two 20 minute changes in fresh xylene, then rehydration in an ethanol series. After this step, slides were processed for antigen

retrieval using a proprietary reagent (Diva Decloaker: Biocare) in a rapid heat procedure using a programmable pressure cooker. This was followed by a 20-minute blocking step using 2.5% horse serum. The primary antibody (diluted in 1.25% horse serum) was then applied and slides incubated at 4^0C overnight in a humidified container. Antibody concentrations were optimized in pilot experiments, beginning with concentrations of 0.5, 1.0 and 1.5 µg/ml.

Day Three, excess primary antibodies were removed by washing and biotinylated species-matched secondary antibody applied. After incubation for 1 hour at room temperature, followed by washing with 10% TBST, endogenous peroxidase activity was blocked by 10 minute incubation in TBS containing 3% hydrogen peroxide. Detection was via application of a commercial HRP-Streptavidin reagent (ABC reagent: Vector Laboratories), and incubation at room temperature for 30 minutes to bind to the biotinylated secondary. After washing off excess reagent, the color reaction was performed by application of a diaminobenzidine preparation (Vector Laboratories), and monitoring for development of brown color under the microscope to determine endpoint. The incubation time depended on antibody, antibody concentration, and antigen distribution, with a goal of reaction being adequate in 10-20 minutes without non-specific background development. For a fairly localized antigen like PCNA (labeling nuclei of proliferating cells), a brown section visible by eye was considered likely overstained. After staining, slides were placed in pure H_2O for at least 1 minute to stop the reaction. A brief counterstain was performed with diluted Vector hematoxylin QS (1 part stain, 2 parts water), followed by permanent cover slip placement with Vecta Mount (Vector Laboratories).

The immunohistochemical protocol was repeated for each experimental and control group. As a negative staining control, the protocol was completed omitting the primary antibody application. Sections were evaluated under a light microscope for the presence or the absence of markers within various tissues within the section, including the new mineralized matrix on the radicular dentinal walls, the supporting periodontium (cementum and bone), and for specimens stained with PCNA, the epithelium.

Results:

Trichome stained samples obtained from the previous study (18) were examined to gain an understanding of general histological findings. Group One (Blood clot/No MTA) specimens demonstrated apical inflammatory infiltrate contacting a band of red blood cells in the canal. Along external and pulpal surfaces, resorptive lacunae were detected both on the apical external and pulpal surfaces of the canal wall. The dentin surface was covered with small cells but only small regions of a thin band of mineralized matrix, and the majority of the pulpal wall lacked mineralized matrix.

Group Two (Blood clot/MTA) specimens demonstrated an absence of inflammatory infiltrate and resorption. At the apex, an apparent cellular, mineralized matrix demonstrated continuous contact along external and pulpal root dentin. This matrix was deposited along the apical pulpal wall, extending over 3.5mm coronally. A layer of mineralizing cells overlaid the deposited matrix with cells within this matrix. Group Three (Blood clot/Biodentine) specimens showed similar results to Group Two. Absence of inflammatory infiltrate and resorption was demonstrated in Group Three specimens. Also similar to Group Two, Group Three demonstrated a mineralized matrix

forming at the apex on external and pulpal surfaces of the dentin, lined and embedded with mineralizing cells.

Group Four (MTA/no clot) specimens demonstrated mineralized matrix deposition in apical regions, along with apparent alveolar bone forming within the pulp, continuous with the bone of the periodontium. Group Five (no treatment) specimens demonstrated an absence of both inflammatory infiltrate (within pulp or periapex) and resorptive processes. Normal cellular cementum was present overlying root dentin, normal cellular cementum was detected, along with odontoblasts lining the pulpal canal wall.

To summarize, the blood clot treatment groups and MTA/Biodentine treatment groups demonstrated extensive areas of active hard tissue matrix formation on the canal walls, extending from the apex, with high levels of cell activity. Expression of mineralization markers (DSPP, OCN, OPN, and CAP), transcription factor marker (OSX), and a cell proliferation marker (PCNA) was detected in regions of interest, and was evaluated for expression patterns in each treatment group.

Group One (Blood clot only) specimens provided moderate staining of DSPP marker within osteoblasts and small cells associated with the thin band of mineralized tissue. Weak DSPP staining was detected in cementoblasts and osteocytes, but cementocytes were unstained (Figure 1). Staining for OCN was strong in cementoblasts, cementocytes, osteoblasts, and cells associated with the newly formed pulpal mineralized tissue, but staining for OCN was weak within osteocytes. OPN staining was strong in cementoblasts, osteoblasts, and cells adjacent to the new pulpal

mineralized matrix, but cementocytes and osteocytes were not stained. The staining patterns for CAP, OSX, and PCNA (Figure 2) were the same as for OPN.

Group Two (Blood clot/MTA) specimens showed the same pattern of staining for DSPP Group One (Blood clot only) for cementoblasts, cementocytes, osteoblasts, and osteocytes, and cells embedded in and adjacent to the new pulpal mineralized matrix stained strongly (Figure 3). Similarly, for OCN, OPN, CAP, OSX, and PCNA, cementoblasts, cementocytes, osteoblasts, and osteocytes had the same pattern of staining as Group One (Figure 4). Staining for OCN, OPN (Figure 5), and CAP was strong within the cells embedded and adjacent to the mineralized matrix. OSX (Figure 6) and PCNA stained strongly in the cells adjacent to the mineralized matrix, but they stained weakly in cells embedded in the matrix.

Group Three (Blood clot/Biodentine) specimens stained moderately for DSPP within osteoblasts and cells adjacent to and embedded in the new pulpal mineralized matrix. The DSPP marker stained weakly in root cementoblasts and osteocytes, and no staining was detected in cementocytes. OCN staining was strong in cementoblasts, osteoblasts, and cells adjacent and embedded within the new pulpal mineralized matrix, and weak staining was detected in cementocytes and osteocytes (Figure 7). Strong staining for OPN was detected in cementoblasts, osteoblasts, and cells adjacent to the mineralized matrix, and moderate staining was detected in cells embedded within the matrix. Weak staining of osteocytes and no staining of cementocytes for OPN was observed (Figure 8). CAP (Figure 9) and OSX (Figure 10) stained strongly in cementoblasts, osteoblasts, and cells adjacent to and embedded within the mineralized matrix. Both markers did not stain cementocytes. Weak staining for OSX was detected

in osteocytes, in which no CAP staining was detected. PCNA (Figure 11) stained strongly within cementoblasts, osteoblasts, and cells adjacent to the new mineralized matrix. Weak staining of PCNA was detected in the embedded cells of the matrix, and no staining was detected in cementocytes and osteocytes.

Group Four (MTA/No induced clot) specimens provided weak staining for DSPP in cementoblasts, cementocytes, osteoblasts, and osteocytes. OCN, OPN, CAP (Figure 12), OSX, and PCNA stained strongly in cementoblasts and osteoblasts, and weak OCN, OPN, OSX, and PCNA staining was seen in cementocytes and osteocytes. In this treatment group, cementocytes and osteocytes did not stain for CAP (Figure 11). Group 5 (Canine Control) specimens stained weakly for DSPP in cementoblasts, cementocytes, osteoblasts, and osteocytes, but odontoblasts stained strongly. Odontoblasts and cementoblasts stained strongly for OCN, OPN, CAP, OSX, and PCNA. Cementocytes stained weakly for these markers, except for CAP, which showed moderate staining in cementocytes. Osteoblasts stained strongly for OCN, CAP, OSX, and PCNA, but stained weakly with the OPN marker.

Overall, with the exception of DSPP a strong expression of the selected markers was detected in odontoblasts, root covering cementoblasts, osteoblasts, and cells adjacent to and embedded within the newly formed pulpal mineralized matrix. A comparatively weaker expression of these markers was detected in cementocytes and osteocytes. In contrast, DSPP showed a weak expression within each of these cell types. In the tissue control Group 5, DSPP expression was greater in odontoblasts. Control samples, in which the primary antibody was omitted in the IHC protocol, resulted in no staining within any of the specimen samples (data not shown).

Furthermore, expression patterns were consistent between different animal samples within a group and between cell populations within the samples.

Discussion

The goals of this study were to evaluate this porcine model as a potential animal model for the study of endodontic regenerative treatment, and to compare via immunohistochemical characterization the early cellular and mineralizing events occurring at the apex following therapies using Biodentine and Pro-Root MTA. The treatment groups utilizing MTA or Biodentine in combination with an induced blood clot (Groups 2 and 3), or MTA alone (Group 4) demonstrated extensive areas of active hard tissue matrix formation on the canal walls, extending from the apex, and with high levels of associated cell activity. Mineralization matrix markers (DSPP, OCN, OPN, and CAP), mineralization transcription factor marker (OSX), and a cell proliferation marker (PCNA) were used in order to characterize this hard tissue matrix along with the associated cells.

DSPP is a preproprotein that gives rise to two proteins: dentin sialoprotein (DSP) and dentin phosphoprotein (DPP). The preproprotein DSPP is secreted by odontoblasts, and DSPP is cleaved by proteinases within the extracellular matrix (ECM) into DSP and DPP. Both DSP and DPP are detected in large amounts in dentin ECM, but DSPP is not. (19, 21, 20) DPP is the most abundant non-collagenous protein in dentin, with a unique structure containing large amounts of aspartic acid and phosphoserine. Discovered through in-vitro mineralization studies, it was found that

DPP plays a key role in the initiation and modulation of the process of forming and growing hydroxyapatite crystals in dentin (22, 23, 24). At the mineralization front, DPP promotes initial hydroxyapatite formation by binding to collagen fibrils and orienting mineral crystals during the mineralization process. Therefore, DPP is important in modulating the conversion of predentin to dentin (25, 26).

It was previous thought that DSPP and its cleaved products were tooth specific (27). However, subsequent studies have shown that they are also produced by osteoblasts and are found in bone, although expressed at much lower levels compared to dentin and odontoblasts (28, 29). A study on rat periodontium detected high levels DSPP in odontoblasts, but weak expression in osteoblasts, cementoblasts, cementocytes, and cells buried in cellular cementum (30). In a rat model, it was demonstrated that DSP was expressed in cellular cementum lining the outside of the root adjacent to the periodontal ligament, but not in acellular cementum in the same regions (34). In the present study, a weaker staining was observed for DSPP within cells adjacent to and embedded within the mineralized tissue lining the apical canal wall. The staining of this mineralized tissue was consistent with the weaker staining seen within cementoblasts, osteoblasts, and osteocytes (Figure 1, Figure 3). The strong staining of odontoblasts in the canine control is consistent with previous studies regarding DSPP expression. The weak DSPP expression pattern within the cells associated with the newly mineralized tissue was therefore not consistent with the strong staining seen in odontoblasts or extracellular matrix within the canine control, in which continuous eruption provides active odontoblasts to observe. Thus, consistent

with the histological appearance, it is unlikely that the newly formed matrix is dentin produced by odontoblasts.

OCN, also known as Bone γ-carboxyglutamic acid (Gla) protein, is produced by osteoblasts, and is one of the most abundant non-collagenous protein component of bone (31). Human OCN is a 46-50 amino acid single chain protein containing three vitamin K-dependent γ- carboxyglutamic acid residues (31). OCN appears transiently in embryonic bone at the time of mineral deposition, where it binds to hydroxyapatite in a calcium-dependent manner (32). Furthermore, many noncollagenous proteins, including OCN, are secreted by odontoblasts associated with the mineralization process of dentin extracellular matrix (33).

OCN expression has been reported in cementoblasts. Previously, it was considered that OCN was only involved in the mineralization process of cellular cementum (34). However, studies on rat periodontium detected OCN expression within cells associated with the mineralization of both cellular cementum and acellular cementum (35). In the present study, the cells adjacent to and embedded within the new hard tissue matrix lining the pulpal canal walls presented with strong expression of OCN. OCN was weakly expressed within cementocytes and osteocytes, but a stronger expression was observed within osteoblasts, odontoblasts, and cementoblasts adjacent to cellular cementum (Figure 4, Figure 6). This strong expression of OCN in these cells is consistent with strong expression within various cells involved in active mineralization, but consequently OCN expression does not provide a specific phenotypic characterization of the pulpal matrix forming cells in this study.

The OPN primary amino acid sequence contains an arginine-glycine-aspartate tripeptide and polyaspartic acid motifs that allows it to serve as a bridge between cells and hydroxyapatite (36). OPN is present in large quantities within bone, but it is also expressed in various other cells and tissues (37, 38), and this diverse expression of OPN represents its multiple functions within various biologic processes. Under physiological conditions, only small amounts of OPN are expressed in the ECM of dentin (39). Within mineralized tissues, OPN acts as an effective inhibitor of hydroxyapatite formation and growth (40, 41). Furthermore, pulp fibroblasts have been found to express OPN, even in various nonmineralized connective tissues (42). This is consistent with observation of samples in this stained for OPN, in which granulation tissue stained stronger compared to other markers (Figure 5, Figure 8).

OPN expression has been reported in cementoblasts. It was previously not considered to be expressed in cells secreting acellular cementum, but subsequent studies have shown that OPN is expressed in cells secreting both cellular and acellular cementum (43). In the present study, strong OPN staining was seen in cells adjacent to and embedded within the hard tissue matrix lining the apical canal walls. Osteoblasts, odontoblasts, and cementoblasts expressed OPN strongly compared to a weaker expression in cementocytes and osteocytes (Figure 5, Figure 8). The results are consistent with expression of OPN in various cells involved in mineralization (eg. cementoblasts, osteoblasts), but the OPN expression pattern within these cells does not provide a specific phenotypic characterization of the cells forming the new pulpal mineralized matrix.

CAP plays a role in the recruitment and differentiation of cells that contribute to cementum formation, and this protein binds to hydroxyapatite and regulates the crystal nucleation in order form cementum (44). CAP is encoded by and is an alternatively spliced transcript of the protein tyrosine phosphatase-like A (PTPLa) gene, which is involved in inducing bone repair and healing (45). CAP is collagen-like, but distinct from collagens type I, XII, and XIV. The ability of CAP to facilitate attachment of various periodontal cells is mediated by integrin receptors on cell surfaces (46). Furthermore, CAP has been found to possess the ability to recruit cementoblastic populations on root slices in-vitro, indicating an important role in cementogenesis during periodontal wound healing (46).

CAP is expressed by cementoblasts, and some previous studies indicated that CAP is specifically expressed only by cementoblasts (47, 48). However, other studies (44, 49) have shown that CAP is expressed by both cementoblasts and osteoblasts, and CAP is also involved in the binding of cells to dentin (50). Therefore, CAP is not considered a specific marker for cementum or cementoblasts. In the current study, CAP was strongly expressed in the cells adjacent to and embedded within the hard tissue located along the apical canal wall. Furthermore, strong staining for CAP was seen in osteoblasts, cementoblasts, and odontoblasts (Figure 9, Figure 12, Figure 13). These results are consistent with expression of CAP within various cells involved with mineralization, but as seen for OCN and OPN, the CAP expression pattern did not provide specific phenotypic characterization of the cells involved in production of the new mineralized matrix. However, the strong expression of CAP in the cells associated

with formation of this matrix would be consistent with its histological appearance as cementum.

OSX is a zinc finger-containing transcriptional activator that is distinctly expressed in all developing bones and is important for osteoblast differentiation. In particular, OSX is implicated in the differentiation of osteoblasts, the specialized cells of bone formation. OSX is a nuclear protein that binds to GC box promoter elements and activates mRNA synthesis from genes containing functional recognition sites (51). As demonstrated in a mouse model, the absence of OSX expression resulted in no cortical or trabecular bone formation, regardless of whether through intramembranous or endochondral ossification. Therefore, OSX functions as a key regulator in the process of bone formation (51).

OSX expression has been detected in osteoblasts (50), cementoblasts, and odontoblasts (52). Similar to osteoblasts, and consistent with the results reported here, cementoblasts express genes for key molecules in mineralization of extracellular matrices, including BSP, OCN, and OPN. Therefore, the OSX transcription factor plays a key role in the process of not only osteogenesis, but also cementogenesis during tooth development (53). Furthermore, a study using mouse odontoblast-like cells found that overexpression of OSX resulted in increased DSPP transcription, providing evidence OSX facilitates the mineralization of dentin ECM (54). Therefore, OSX is not specific for a single type of cell involved in mineralization, but labels osteoblasts, cementoblasts, or odontoblasts.

Studies have demonstrated the mesenschymal origin of cellular cementum from cementoblasts arising a lineage from periodontal ligament progenitor cells (55). OSX expression in cementoblasts has been studied in regards to its temporal- and spatial-expression pattern during the formation of cellular cementum (55). Deleting OSX expression in mice resulted in a large reduction in cellular bone formation (including the overall mass and rate of formation), and furthermore, OSX transgenic mice demonstrated an accelerated and increase of cellular cementum formation. However, deletion of OSX expression did not alter mature cementum properties (56). Therefore, in regards to cellular cementum formation, OSX is a key regulator of the transcription of molecules involved in mineralization during the early phases of cementogenesis in cellular cementum formation. In the current study, strong OSX expression was detected on the cells adjacent to the hard tissue matrix located on the apical canal. In regards to the cells embedded within this hard tissue matrix, some of these cells expressed OSX and some did not. Furthermore, osteocytes did not express significant levels of OSX, while pronounced expression of OSX was detected within cementoblasts and osteoblasts (Figure 7, Figure 10). These results indicate possible active mineralization by cells adjacent to and embedded within hard tissue matrix, and these results are consistent with evidence for cellular cementum characteristics. However, OSX is not a specific marker for cementoblasts, and therefore, the definitive recognition of the matrix and associated cells cannot be determined based solely on OSX expression pattern.

The proliferating cell nuclear antigen (PCNA) is a protein synthesized in early G1 and S phases of the cell cycle, and PCNA provides functions in cell cycle progression, DNA replication and DNA repair (57). PCNA expression can be detected in oral

epithelium and mesenchyme, before any signs of dental lamina formation (i.e. before the tooth bud formation stage begins). Throughout the bud, cap, and bell stages, PCNA expression can be found at certain sites within the enamel organ, dental papilla, and dental follicle. Therefore, PCNA is a reliable marker for proliferating cells associated with tooth formation (57). PCNA expression labels cells that are within any phase of the cell cycle, but the expression or staining pattern varies according to the cell cycle phase of the proliferating cell. There is relatively no expression of PCNA during the G0-phase, followed by a slight rise of PCNA expression in the early G1-phase. During the late G1- and early S-phases, there is a prominent rise in expression of PCNA, with the maximum expression detected during the late S-phase (57, 59).

PCNA is expressed in numerous cells throughout the body, including fibroblasts, ameloblasts, odontoblasts, and cementoblasts (60, 61). PCNA expression is prominent in cells within the enamel organ and dental papilla during dentinogenesis and cementogenesis (60). Therefore, PCNA expression is not specific to any particular mineralization process; the patterns of expression identify whether populations are actively dividing (as expected in regenerating tissues). In the current study, strong PCNA expression was observed within the nuclei of cells adjacent to the hard tissue matrix located along the apical canal wall, but PCNA expression was not detected within the cells embedded within the hard tissue matrix. Furthermore, PCNA expression was detected within osteoblasts and cementoblasts (identified by location), but not within osteocytes. This PCNA expression pattern provided evidence for actively dividing cells associated with the secretion of the hard tissue matrix along the apical canal wall

(Figure 2). As a positive control, PCNA expression was detected in the oral epithelial tissues, specifically the basal layer of cells (Figure 11).

Presently, there are no known dentin-specific, cementum-specific, or bone specific proteins, and cells involved in different mineralization processes broadly secrete the same proteins. The main distinction between these different mineralized matrices (dentin, cementum, and bone) is based on quantitative amounts of individual proteins within the mineralized matrix, and such quantification is challenging using immunohistochemistry. Furthermore, comparisons using immunohistochemical quantification are further limited when the sample size is small, as in the current study. Therefore, the results from this study with the selected markers must be considered in aggregate, and by comparison with results of marker expression in internal and known control tissues, including dentin, cementum, bone, and epithelium. The expression pattern of the markers within the cells observed adjacent to and embedded in the mineralized matrix were therefore compared to these control tissues within the same immunohistochemically stained sample.

Previous studies using histochemical staining in this model indicated that the mineralized tissue forming along the internal canal walls appeared to be comprised of either cementum-like or osteoid-like tissues, or perhaps even a mixture of the two. Therefore, in this study, an immunohistochemical evaluation with select markers was used in an effort to distinguish the phenotypic characteristics of the mineralized hard tissue and the cells associated with its formation. The expression pattern of the mineralization markers DSPP, OCN, OPN, and CAP described here provided evidence that the mineralized tissue resembles cellular cementum, and is most likely not dentin.

However, there is still the challenge presented by the expression of these markers in multiple mineralizing cell types, with no marker specific to cementoblasts, because each mineralization marker has the potential to be expressed by cementoblasts, odontoblasts, or osteoblasts. The transcription factor marker OSX has a similar limitation, but it can be used to provide evidence for the presence of cellular cementum versus acellular cementum. Overall, it is not possible to determine definitively if the mineralized tissue is dentin, cementum, or bone, but the evidence in total indicated the formation of a cellular cementum-like tissue adjacent to cementoblast-like cells along the internal canal wall.

This porcine model has demonstrated similar results to those from human studies and other animal studies. Small and large animal models have been evaluated histologically following regenerative endodontic therapies, but many animals have limitations in research. Canine (dog) models provide large teeth, comparable to humans, but these models are expensive and also present with ethical concerns in many regions of the world. Also smaller animal models, like ferrets or mice, make treatment difficult and are technique sensitive in regards to executing reliable regenerative endodontic treatment. The porcine model utilized in this study presents with fewer ethical concerns and is more affordable, and furthermore, young pigs have a similar tooth morphology and size compared to human teeth with immature roots. As demonstrated in this current study, the porcine model shows promise for the further investigation of the cellular events involved in the regeneration of mineralized tissue in teeth that have undergone regenerative endodontic therapy.

References

1. Hargreaves K, Diogenes A, Texixeira F. Treatment Options: Biological Basis of Regenerative Endodontic Procedures. J Endod 2013: 39; S30-43.
2. Murray P, Garcia-Godoy F, Hargreaves F. Regenerative Endodontics: A Review of Current Status and a Call for Action. J Endod 2007: 33; 377–90.
3. de Silva LA, Nelson-Filho P, da Silva RA, et al. Revascularization and periapical repair after endodontic treatment using apical negative pressure irrigation versus conventional irrigation plus triantibiotic intracanal dressing in dogs' teeth with apical periodontitis. Oral Surg Oral Med Oral Pathol Oral Radiol Endod 2010; 109: 779–87.
4. Wang X, Thibodeau B, Trope M, Lin LM, Huang GT. Histologic characterization of regenerated tissues in canal space after the revitalization/revascularization procedure of immature dog teeth with apical periodontitis. J Endod 2010; 36: 56–63.
5. Andreasen JO, Bakland LK. Pulp regeneration after non-infected and infected necrosis, what type of tissue do we want? A review. DentTraumatol 2012; 28: 13–8.
6. Martin DE, De Almeida JF, Henry MI. Concentration-dependent effect of sodium hypochlorite on stem cells of apical papilla survival and differentiation. J Endod 2014; 40: 51–5.
7. Meschi N, Hilkens P, Lambrichts I. Regenerative endodontic procedure of an infected immature permanent human tooth: an immunohistological study. Clinical Oral Investigations 2015 [Epub ahead of print].
8. KM Hargreaves, T Geisler, M Henry, Y Wang. Regeneration potential of the young permanent tooth: what does the future hold? J Endod, 2008; 34: S51-S56.

9. Konstantinos Stellos, Sebastian Kopf, Angela Paul, Jens U. Marquardt, Meinrad Gawaz, Johnny Huard, Harald F. Langer. Platelets in regeneration. Semi Thromb Hemost. 2010; 36: 175-184.
10. Zanini M, Sautier JM, Berdal A, Simon S. Biodentine induces immortalized murine pulp cell differentiation into odontoblast-like cells and stimulates biomineralization. J Endod. 2012; 38: 1220-6.
11. Parirokh M, Torabinejad M. Mineral trioxide aggregate: a comprehensive literature review—part I: chemical, physical, and antibacterial properties. J Endod. 2010; 36:16-27.
12. Torabinejad M, Parirokh M. Mineral trioxide aggregate: a comprehensive literature review—part II: leakage and biocompatibility investigations. J Endod. 2010; 36: 190-202.
13. Kontakiotis E, Filippatos CG, Agrafioti A. Levels of Evidence for the Outcome of Regenerative Endodontic Therapy. Review Article. J Endod 2014; 40: 1045–1053.
14. Bose R, Nummikoski P, Hargreaves K. A retrospective evaluation of radiographic outcomes in immature teeth with necrotic root canal systems treated with regenerative endodontic procedures. J Endod 2009; 35:1343–9.
15. Jeeruphan T, Jantarat J, Yanpiset K, et al. Mahidol study 1: comparison of radiographic and survival outcomes of immature teeth treated with either regenerative endodontic or apexification methods—a retrospective study. J Endod 2012; 38: 1330–6.
16. Swindle M, Smith A. Swine in the Laboratory: Surgery, Anesthesia, Imaging, and Experimental Techniques, Third Edition. Boca Raton, FL: CRC Press 2007.

17. Hargreaves JA, Mitchell B. Features of the dentition of the pig for experimental work. J. Dent. Res. 1969; 48: 1103.
18. Lane A, Evaluation of a Porcine Model for Exploration of Endodontic Regeneration Strategies Using Mineral Trioxide Aggregate and Biodentine. Uniformed Services University of the Health Sciences. 2016.
19. MacDougall M, Simmons D, Luan X, Nydegger J, Feng J, Gu TT. Dentin phosphoprotein and dentin sialoprotein are cleavage products expressed from a single transcript coded by a gene on human chromosome 4. Dentin phosphoprotein DNA sequence determination. J Biol Chem. 1997; 272: 835-842.
20. Gu K, Chang S, Ritchie HH, Clarkson BH, Rutherford RB. Molecular cloning of a human dentin sialophosphoprotein gene. Eur J Oral Sci 2000; 108: 35-42.
21. Ritchie HH, Wang LH, Knudtson K. A novel rat 523 amino acid phosphophoryn: Nucleotide sequence and genomic organization. Biochim Biophys Acta. 2001; 1520: 212-222.
22. Unde A, Lussi A, Crenshaw MA. Mineral induction by immobilized polyanionic proteins. Calcif Tissue Int. 1989; 44: 286-295.
23. Boskey AL, Maresca M, Doty S, Sabsay B, Veis A. Concentration-dependent effects of dentin phosphophoryn in the regulation of in vitro hydroxyapatite formation and growth. Bone Miner. 1990; 11: 55-65.
24. Saito T, Arsenault AL, Yamauchi M, Kuboki Y, Crenshaw MA. Mineral induction by immobilized phosphoproteins. Bone. 1997; 21: 305-311.
25. Linde A, Goldberg M. Dentinogenesis. Crit Rev Oral Biol Med 1993; 4: 679-728.

26. Butler WT, Ritchie H. The nature and functional significance of dentin extracellular matrix proteins. Int J Dev Biol 1995; 39: 169-179.
27. Butler WT. Dentin matrix proteins. Eur J Oral Sci 1998; 106: 204-210.
28. Qin C, Brunn JC, Cadena E, et al. The expression of dentin sialophosphoprotein gene in bone. J Dent Res 2002; 81: 392-394.
29. Qin C, Brunn JC, Cadena E, Ridall A, Butler WT. Dentin sialoprotein in bone and dentin sialophosphoprotein gene by osteoblasts. Connect Tissue Res 2003; 44: 179-183.
30. Baba O, Qin C, Brunn JC, et ai. Detection of dentin sialoprotein in rat periodontium. EurJ Oral Sci 2004; 112: 163-170.
31. Kasai, R., et al. 1994. Production and characterization of an antibody against the human bone GLA protein (BGP/osteocalcin) propeptide and its use in immunocytochemistry of bone cells. Bone Miner. 25: 167-182.
32. Chenu, C., et al. 1994. Osteocalcin induces chemotaxis, secretion of matrix proteins and calcium-mediated intracellular signaling in human osteoclastlike cells. J. Cell Biol. 127: 1149-1158.
33. Goldberg M, Smith AJ. Cells and extracellular matrices of dentin and pulp: A biological basis for repair and tissue engineering. Crit Rev Oral Biol Med 2004; 15: 13-27.
34. Bronkers, ALJJ, Farach-Carson MC, Waveren EV, Butler WT. Immunolocalization of osteopontin, osteocalcin, and dentin sialoprotein during root formation and early cementogenesis in the rat. J Bone Min Res 1994; 9: 833-41.

35. Tenorio D, Cruchley, A, Hughes FJ. Immunocytochemical investigation of the rat cementoblast phenotype. J Periodont Res 1993; 28: 411-19.
36. Olderberg A, Franzen A, Heinegard D. Cloning and sequence analysis of rat bone sialoprotein (osteopontin) cDNA reveals an Arg-Gly-Asp cell-binding sequence. Proc Natl Acad Sci USA 1986; 83: 8819-8823.
37. Noda M, Denhardt DT. Osteopontin. In: Bilezikian JP, Raisz LG, Martin TJ (eds). Principles of Bone Biology, vol 1, ed 3. San Diego: Academic Press, 2008:351 366.
38. Sodek J, Ganss B, McKee MD. Osteopontin. Crit Rev Oral Biol Med 2000; 11: 279-303.
39. Qin C, Brunn JC, Jones J, et al. A comparative study of sialic acid-rich proteins in rat bone and dentin. EurJ Oral Sci 2001; 109: 133-141.
40. Boskey AL, Maresca M, Ullrich W, Doty SB, Butler WT, Prince CW. Osteopontin-hydroxyapatite interactions in vitro: Inhibition of hydroxyapatite formation and growth in a gelatin-gel. Bone Miner 1993; 22: 147-159.
41. Boskey AL, Spevak L, Paschalis E, Doty SB, McKee MD. Osteopontin deficiency increases mineral content and mineral crystallinity in mouse bone. Calcif Tissue Int 2002; 71: 145-154.
42. Yokota M, Nagata T, Ishida H, Wakano Y. Clonal dental pulp cells (RDP4-1, RPC-C2A) synthesize and secrete osteopontin (SPP1, 2ar). Biochem Biophys Res Commun 1992; 189: 892-898.
43. Hirata A, Sugahara T, Nakamura H. Localization of Runx2, Osterix, and Osteopontin in Tooth Root Formation in Rat Molars. Journal of Histochemistry and Cytochemistry. 2009; 57: 397–403.

44. Montoya G, Arenas J, Romo E, Zeichner-David M, Alverez, Narayanan A, Velazquez U, Mercado G, Arzate H. Human recombinant cementum attachment protein (hrPTPLa/CAP) promotes hydroxyapatite crystal formation in vitro and bone healing in vivo. Bone. 2014; 69: 154-164.
45. Schild C, Beyeler M, Lang N, Trueb B. Cementum attachment protein/protein-tyrosine phosphotase-like member A is not expressed in teeth. International Journal of Molecular Medicine. 2008; 23: 293-296.
46. Barkana I, Narayanan AS, Grosskop A, Savion N, Pitaru S. Cementum Attachment Protein Enriches Putative Cementoblastic Populations on Root Surfaces in vitro. Journal of Dental Research. 2000; 79: 1482-1488.
47. Arzate H, Olson SW, Page RC, Gown AM and Narayanan AS. Production of a monoclonal antibody to an attachment protein derived from human cementum. FASEB J 6. 1992: 2990-95.
48. Saito M, Iwase M, Maslan S, Nozaki N, Yamauchi M, Handa K, Takahashi O, Sato S, Kawase T, Teranaka T and Narayanan AS. Expression of cementum-derived attachment protein in bovine tooth germ during cementogenesis. 2001. Bone 29: 242-248.
49. Liu WL, Rinat Y, Savion N, Narayanan AS, Pitaru S. A Collagenous Cementum-Derived Attachment Protein Is a Marker for Progenitors of the Mineralized Tissue-Forming Cell Lineage of the Periodontal LigamentJournal of Bone and Mineral Research. 1997; 12: 1691-99.

50. Pitaru S, Savion N, Hekmati H, Olsen S, Narayanan SA. Binding of a cementum attachment protein to extracellular matrix components and to dental surfaces. J Periodontal Res. 1992; 27: 640-6.
51. Nakashima, K. Zhou X, Kunkel G, Zhang Z, Deng JM, Behringer RR, de Crombrugghe B. The novel zinc finger-containing transcription factor osterix is required for osteoblast differentiation and bone formation. Cell. 2002; 108: 17-29.
52. Wang C, Liao H, Cao Z. Role of Osterix and MicroRNAs in Bone Formation and Tooth Development. Med Sci Monit. 2016; 22: 2934-2942
53. Hirata A, Sugahara T, Nakamura H: Localization of runx2, osterix, and osteopontin in tooth root formation in rat molars. J Histochem Cytochem, 2009; 57(4): 397–403
54. Chen S, Gluhak-Heinrich J, Wang YH. Runx2, osx, and dspp in tooth development. J Dent Res. 2009; 88: 904–9.
55. Cao Z, Zhang H, Zhou X. Genetic evidence for the vital function of Osterix in cementogenesis. J Bone Miner Res. 2012; 27: 1080–92.
56. Liu R, Cao Z. Osterix combined with gene-activated matrix: A potential integrated strategy for achieving cementum regeneration. Dent Hypotheses. 2015. 6: 10–13.
57. Kurki P, Vanderlaan M, Dolbeare F, Gray J, Tan EM. Expression of proliferating cell nuclear antigen (PCNA)/cyclin during the cell cycle. Exp Cell Res. 1986; 166: 209-19.
58. Matulová P1, Witter K, Mísek I. Proliferating cell nuclear antigen (PCNA) expression in tooth primordia in the field vole (Microtus agrestis, Rodentia). Connect Tissue Res. 2002; 43:138-42.

59. Kelman Z. PCNA: structure, functions and interactions. Oncogene. 1997; 14: 629-40.

60. Zhao S1, Jin Y, Li S, Zhao M, Yang X. Cell proliferation and programmed cell death in tooth development. Hua Xi Kou Qiang Yi Xue Za Zhi. 1999; 17: 99-101.

61. Ebensberger U, PohlY, Filippi A. PCNA-expression of cementoblasts and fibroblasts on the root surface after extraoral rinsing for decontamination. Dent Traumatol. 2002; 18: 262-266.

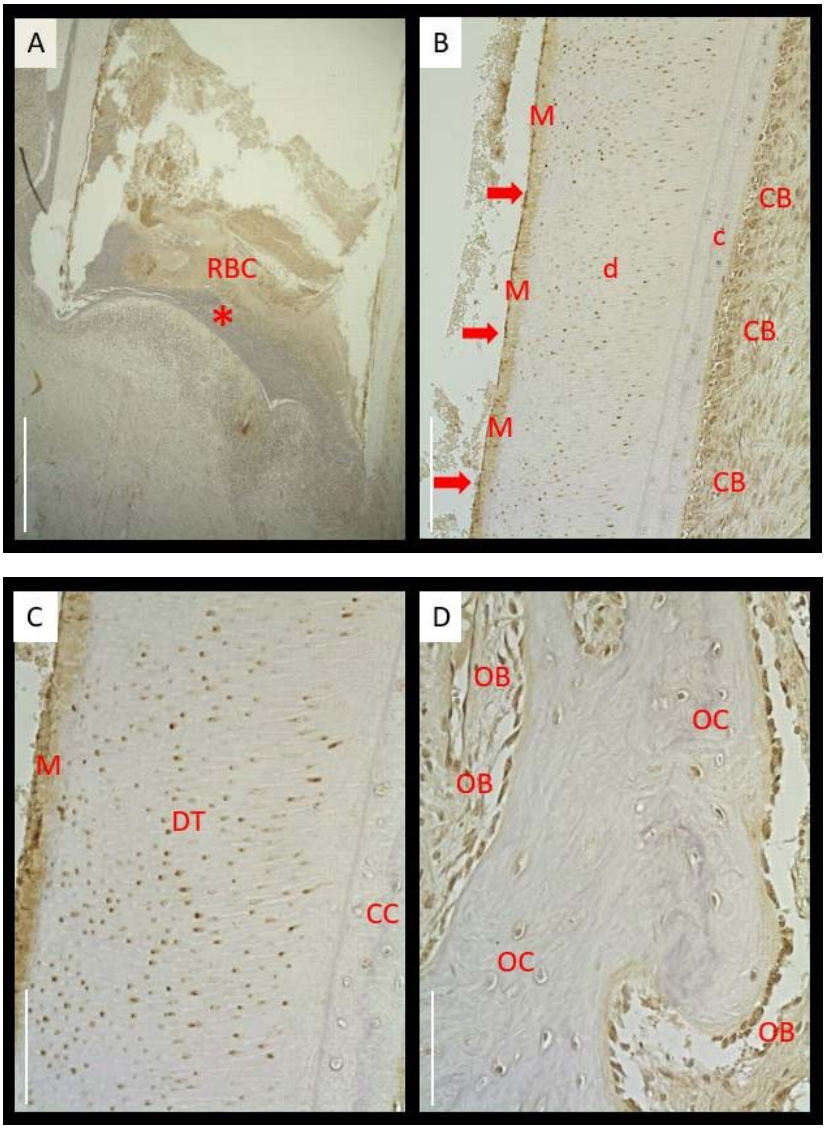

Figure 1: Group 1 **(A)** Representative sample of apex (star) of a FUJI and blood clot treated premolar stained with DSPP marker. The specimen demonstrated a prominent inflammatory infiltrate (star) at the apex contacting a band of red blood cells (RBC) in the canal; the rest of the canal was largely empty of any other tissues and cells (4x magnification, scale bar = 1 mm). **(B)** Dentin surface (d) covered with small cells, moderately stained with DSPP adjacent to weakly stained regions of newly formed pulpal mineralized matrix (M). Weak DSPP staining of cementoblasts (CB) lining cementum (c) of external root surface. (20x magnification, scale bar = 200µm) **(C)** Higher magnification of mineralized tissue (M). Dentinal tubules (DT) present with moderate staining. There is a lack of DSPP staining of cementocytes (CC) on external surface of root (40x magnification, Scale bar =100µm). **(D)** Moderate DSPP staining of osteoblasts (OB) lining bone of periodontium with weak staining of embedded osteocytes (OC) (40x Magnification, Scale bar =100µm).

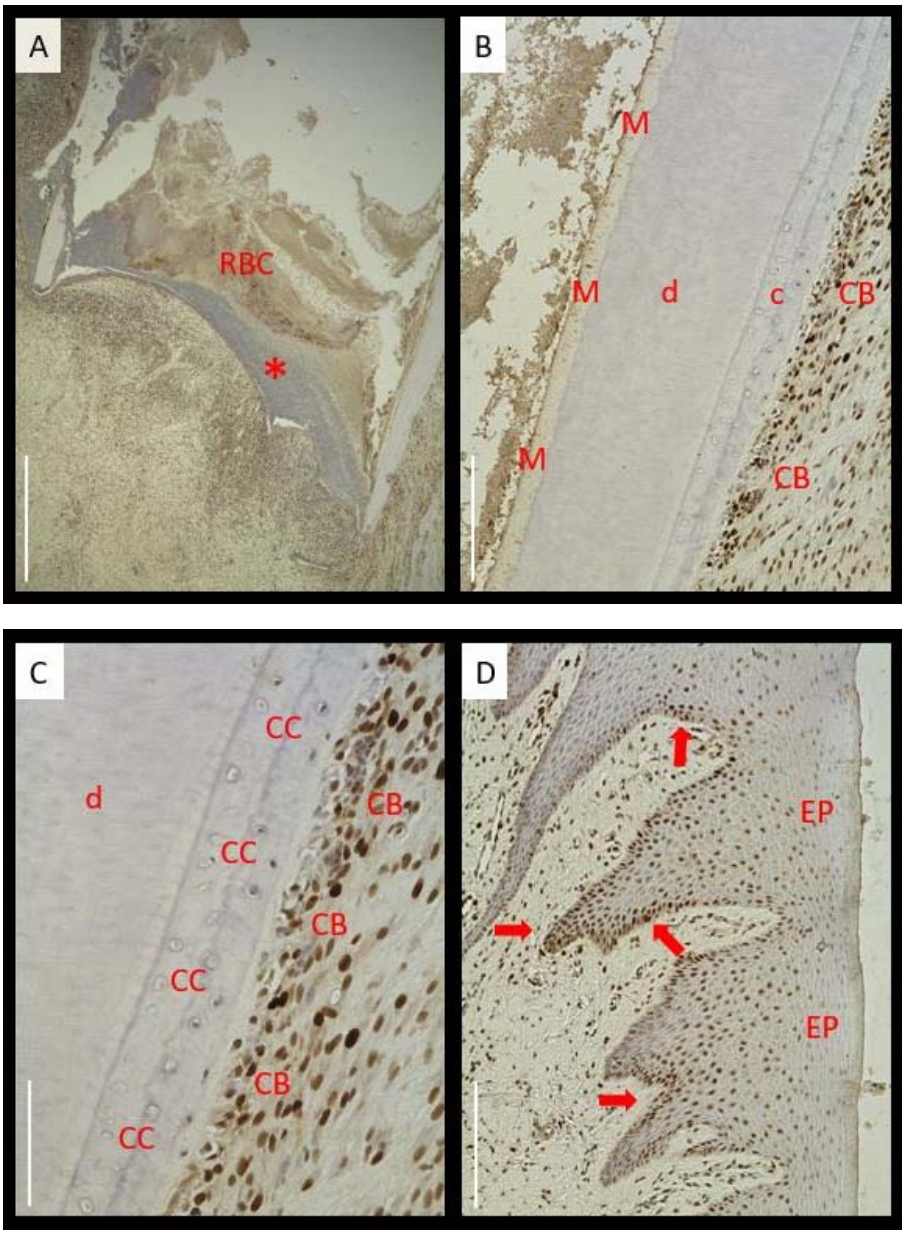

Figure 2: Group 1 **(A)** Representative sample of apex of a FUJI and blood clot treated premolar stained with PCNA marker. The specimen demonstrated a prominent inflammatory infiltrate (star) at the apex contacting a band of red blood cells (RBC) in the canal; the rest of the canal was largely empty of any other tissues and cells (4x magnification, scale bar = 1 mm). **(B)** At midroot; dentin surface (d) adjacent to regions of mineralized matrix (M). Cementoblasts (CB), strongly stained with PCNA, overlaying cementum (c) (20x magnification, scale bar = 200μm). **(C)** Adjacent to dentin (d), cementum containing embedded, non-stained cementocytes (CC). On external root surface, strongly stained cementoblasts (CB) overlaying cementum (40x magnification, Scale bar =100μm). **(D)** Gingival epithelium (EP) with strongly stained basal layer of epithelial cells (arrows) adjacent to connective tissue (positive control for proliferative

cells). Epithelial staining weakening as epithelial cell migrate to external surface (20x Magnification, Scale bar =200μm).

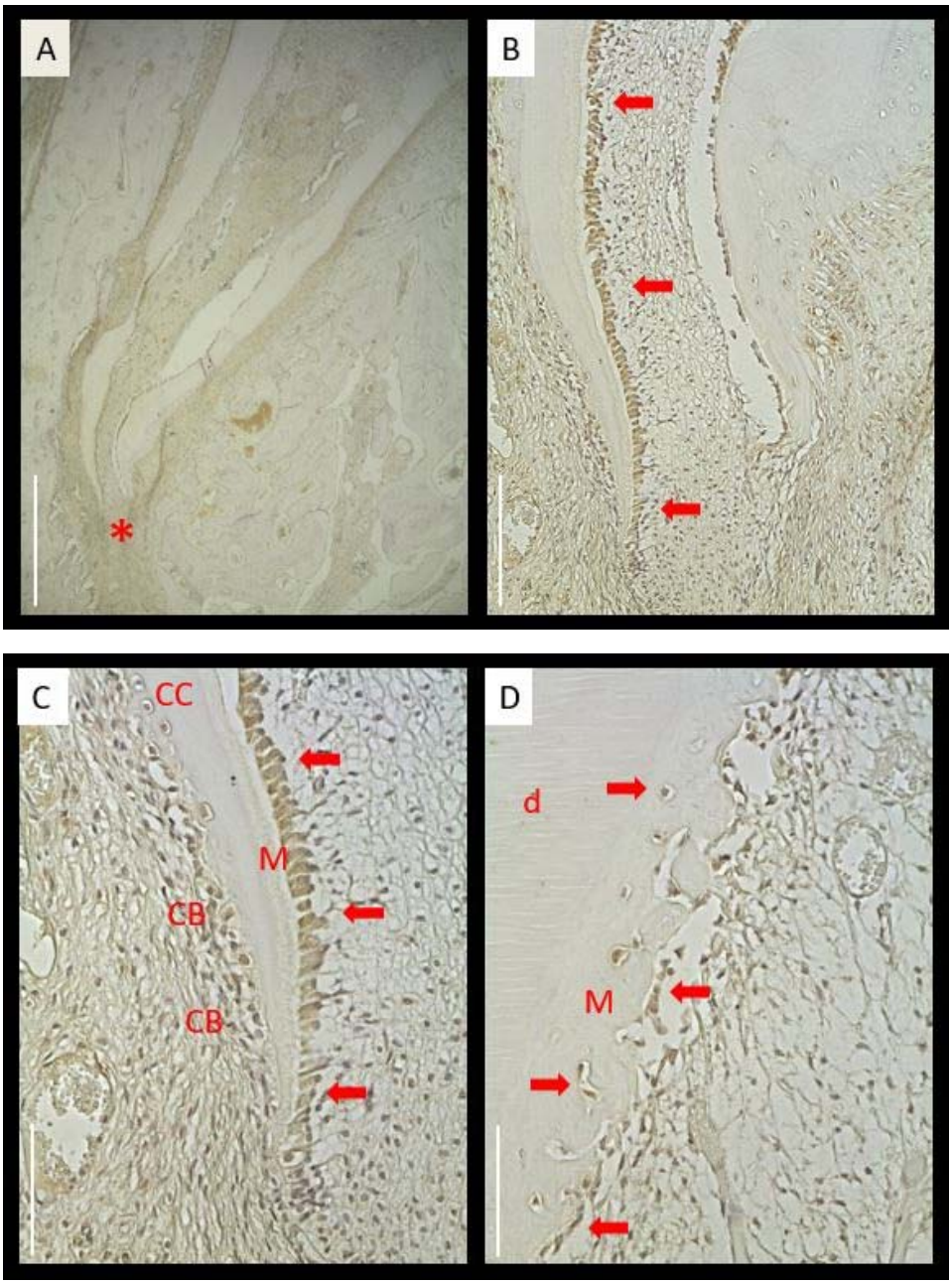

Figure 3: Group 2 **(A)** Representative sample the apex (star) of a MTA and blood clot treated premolar (4x magnification, scale bar = 1 mm). **(B)** Columnar layer of cells (arrows), moderately stained with DSPP lining internal surface of the apex (20x magnification, scale bar = 200μm) **(C)** Magnified columnar layer of cells (arrows) depositing mineralized matrix (M) at apex. Weakly stained cementoblasts (CB) lining external surface of root depositing cementum and weakly stained cementocytes (CC) embedded in cementum (40x magnification, Scale bar =100μm). **(D)** At midroot, a layer of cells (arrows), moderately stained with DSPP, overlaid the deposited matrix (M)

adjacent to dentin (d). Within in the matrix, embedded cells (arrows), stained weakly for DSPP (40x Magnification, Scale bar =100μm).

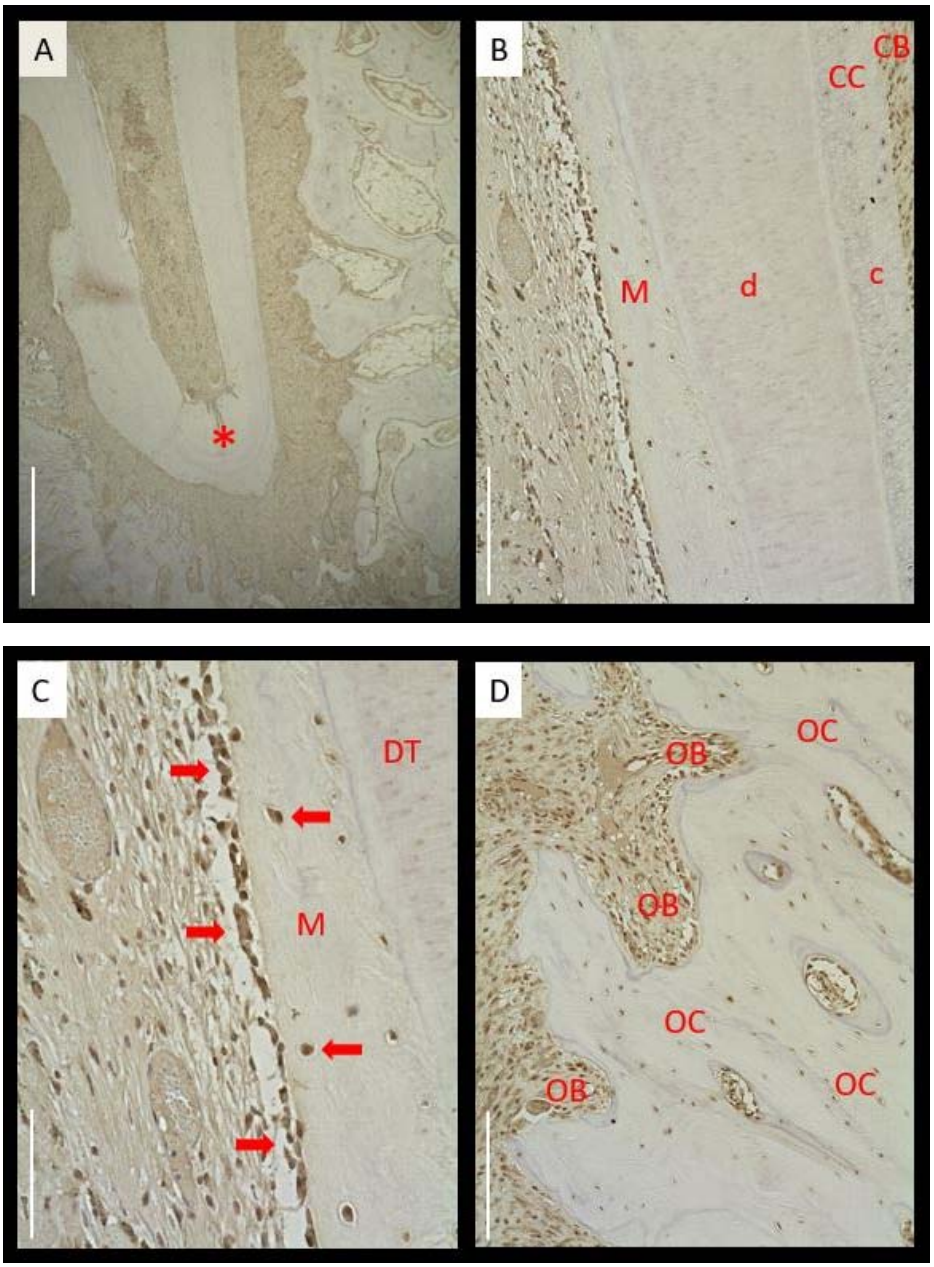

Figure 4: Group 2 **(A)** Representative sample the apex (star) of a MTA and blood clot treated premolar stained for osteocalcin (4x magnification, scale bar = 1 mm). **(B)** Mineralized matrix (M) lining internal surface of the canal wall, adjacent to dentin (d) and cementum (c). Cementoblasts (CB) and cementocytes (CC) strongly stained for osteocalcin lining the external surface of the root. (20x magnification, scale bar = 200μm) **(C)** Layer of cells (arrows), strongly stained for osteocalcin, overlaying the mineralized matrix (M) with strongly stained embedded cells (arrows) within the matrix. Dentinal tubules (DT) stained weakly for osteocalcin (40x magnification, Scale bar =100μm). **(D)** Bone of the supporting periodontium with strong OCN staining detected in

osteoblasts (OB) and weak staining detected in osteocytes (OC) (20x Magnification, Scale bar =200μm).

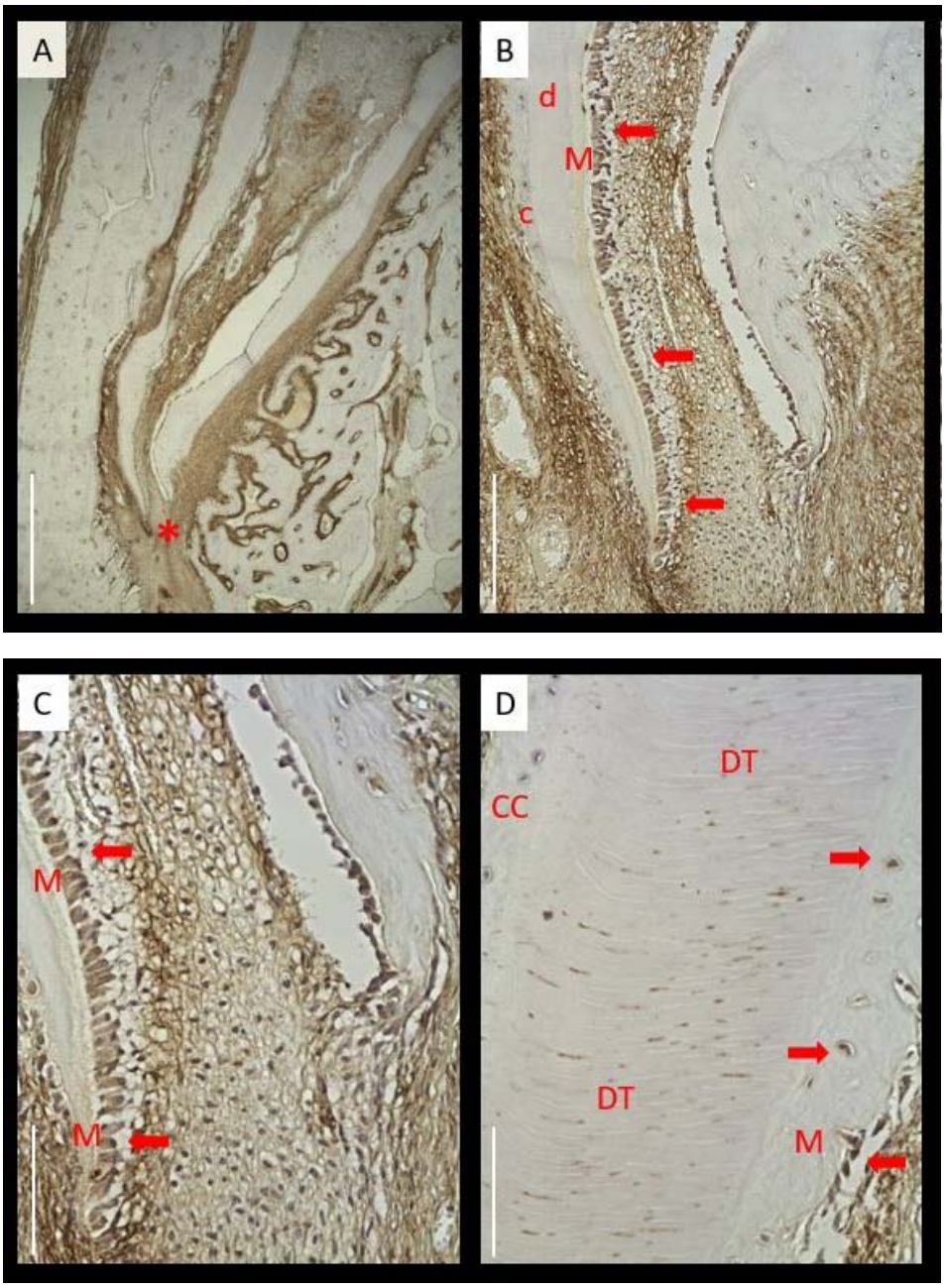

Figure 5: Group 2; **(A)** Representative sample the apex (star) of a MTA and blood clot treated premolar stained with osteopontin marker (4x magnification, scale bar = 1 mm). **(B)** Columnar layer of cells (arrows), strongly stained with osteopontin marker, lining internal surface of the apex and secreting mineralized matrix (M) adjacent to dentin (d) and cementum (c) (lining the external surface of the root) (20x magnification, scale bar = 200μm) **(C)** Magnified columnar layer of cells (arrows) depositing mineralized matrix (M) at apex (40x magnification, Scale bar =100μm). **(D)** At midroot, a layer of cells

(arrow), strongly stained with osteopontin marker, overlaid the deposited matrix (M). Within in the matrix, embedded cells (arrows), strongly stained with osteopontin marker. Cementocytes (CC) not stained, and dentinal tubules (DT) moderately stained (40x Magnification, Scale bar =100µm).

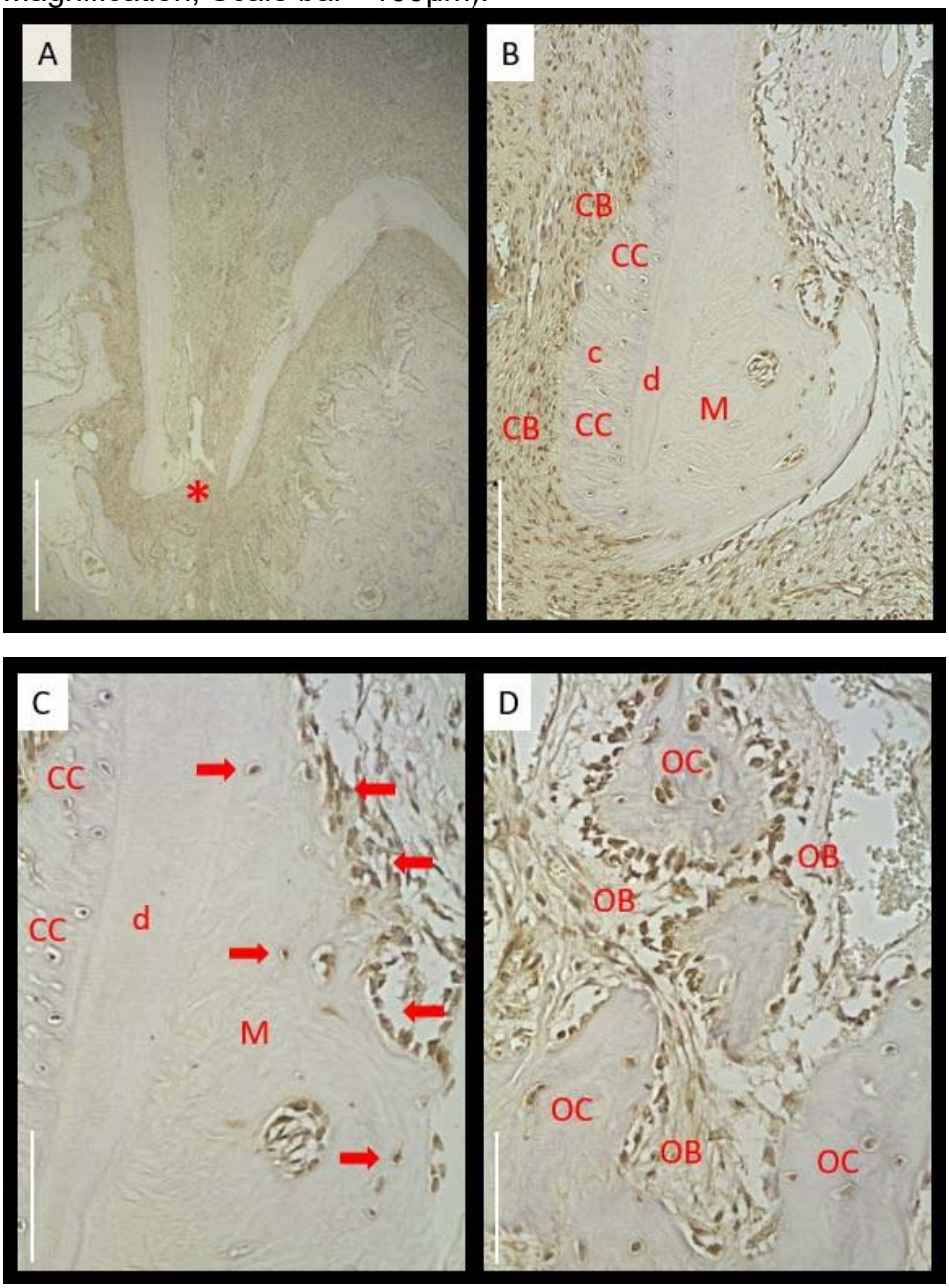

Figure 6: Group 3; **(A)** Representative sample the apex (star) of a Biodentine and blood clot treated premolar stained with osteocalcin marker (4x magnification, scale bar = 1 mm). **(B)** Mineralized matrix (M) lining internal surface of the canal wall, adjacent to dentin (d) and cementum (c). Cementoblasts (CB), strongly stained, and cementocytes (CC), weakly stained, lining the external surface of the root. (20x magnification, scale bar = 200µm) **(C)** Layer of cells (arrows), strongly stained with osteocalcin marker, overlaying the mineralized matrix (M) with strongly stained embedded cells (arrows)

within the matrix. (40x magnification, Scale bar =100μm). **(D)** Bone of the supporting periodontium with strong staining detected in osteoblasts (OB) and weak staining detected in osteocytes (OC) (40x Magnification, Scale bar =100μm).

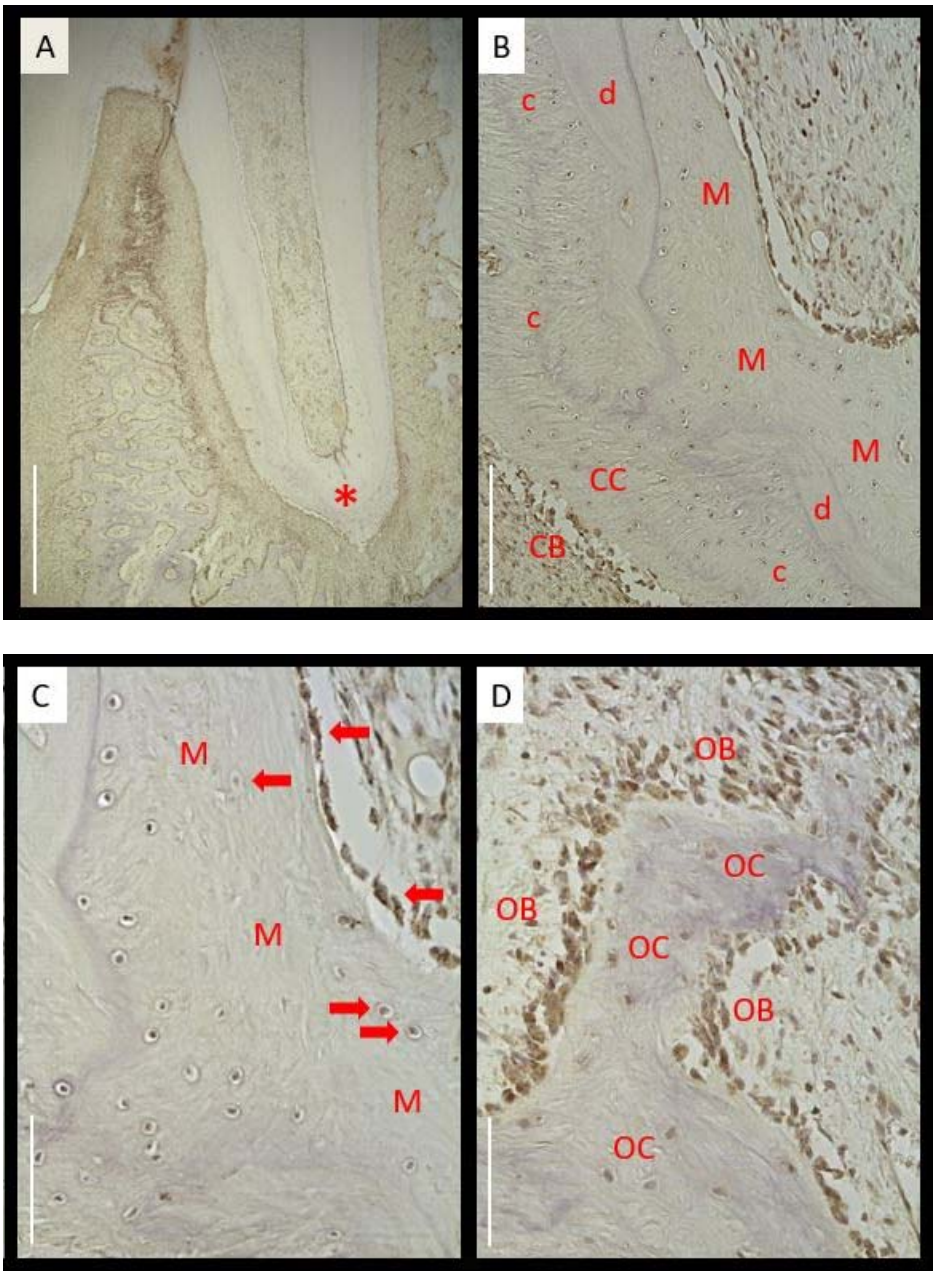

Figure 7: Group 2 **(A)** Representative sample a root and apex (star) of a MTA and blood clot treated premolar stained with osterix marker (4x magnification, scale bar = 1 mm). **(B)** Mineralized matrix (M) lining internal surface of the canal wall, adjacent to dentin (d) and cementum (c). Cementoblasts (CB), strongly stained, and cementocytes (CC), not stained, with osterix marker (lining the external surface of the root) (20x magnification, scale bar = 200μm) **(C)** Layer of cells (arrows), strongly stained,

overlaying the mineralized matrix (M) with weakly stained embedded cells (arrows) within the matrix. (40x magnification, Scale bar =100μm). **(D)** Bone of the supporting periodontium with strong staining detected in osteoblasts (OB) and weak staining detected in osteocytes (OC) (40x Magnification, Scale bar =100μm).

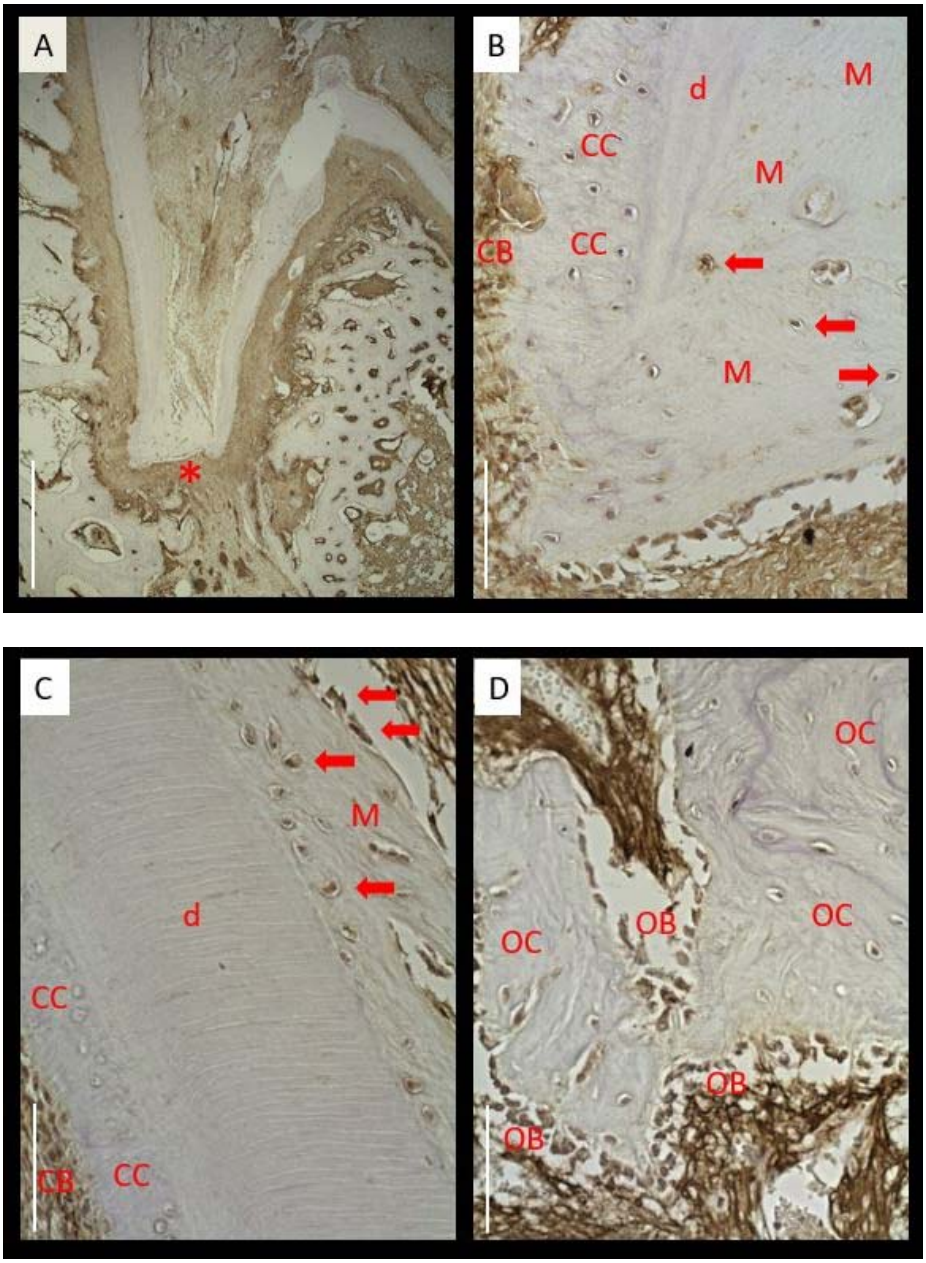

Figure 8: Group 3; **(A)** Representative sample the apex (star) of a Biodentine and blood clot treated premolar stained with osteopontin marker (4x magnification, scale bar = 1 mm). **(B)** Mineralized matrix (M) lining internal surface of the canal wall, adjacent to dentin (d). Within the matrix, embedded cells (arrows) moderately stained. Cementoblasts (CB), strongly stained, and cementocytes (CC), not stained, lining the external surface of the root. (20x magnification, scale bar = 200μm) **(C)** At midroot, layer of cells (arrows), strongly stained with osteopontin marker, overlaying the mineralized

matrix (M) with moderately stained embedded cells (arrows) within the matrix. Cementoblasts (CB), strongly stained, and cementocytes (CC), not stained, lining the external surface of the root (20x magnification, Scale bar =200μm). **(D)** Bone of the supporting periodontium with strong staining detected in osteoblasts (OB) and weak staining detected in osteocytes (OC) (20x Magnification, Scale bar =200μm).

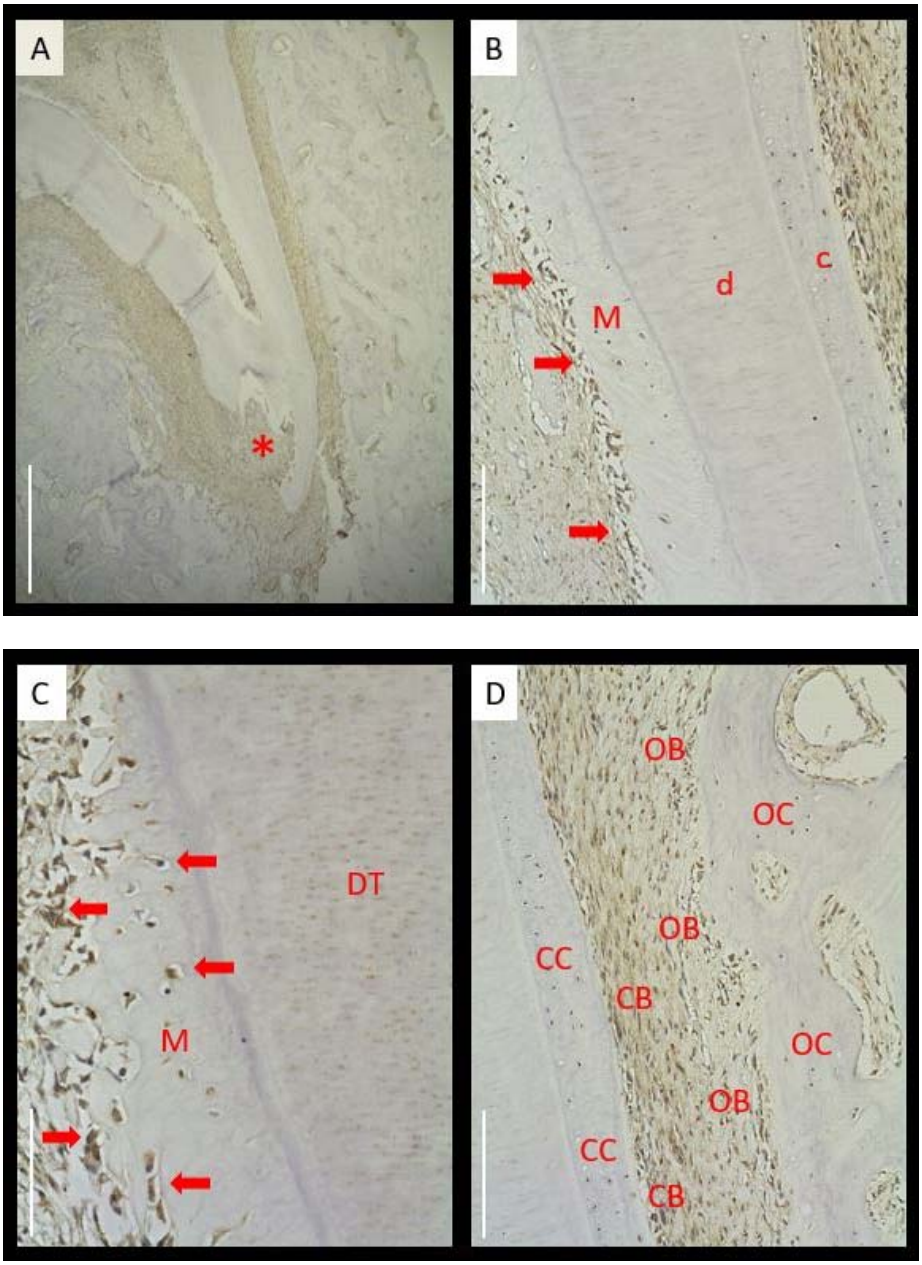

Figure 9: Group 3; **(A)** Representative sample of the root and apex (star) of a Biodentine and blood clot treated premolar stained with CAP marker (4x magnification, scale bar = 1 mm). **(B)** At midroot, a layer of strongly stained cells (arrows) secreting a mineralized matrix (M), lining the internal surface of the canal wall, adjacent to dentin (d) and cementum (c) (20x magnification, scale bar = 200μm). **(C)** At midroot, layer of cells (arrows), strongly stained with CAP marker, overlaying the mineralized matrix (M) with

strongly stained embedded cells (arrows) within the matrix. Dentinal tubules moderately stained by CAP (40x magnification, Scale bar =100μm). **(D)** Cementoblasts (CB), strongly stained, and cementocytes (CC), not stained, lining the external surface of the root. Bone of the supporting periodontium with strong staining detected in osteoblasts (OB) and no staining detected in osteocytes (OC) (20x Magnification, Scale bar =200μm).

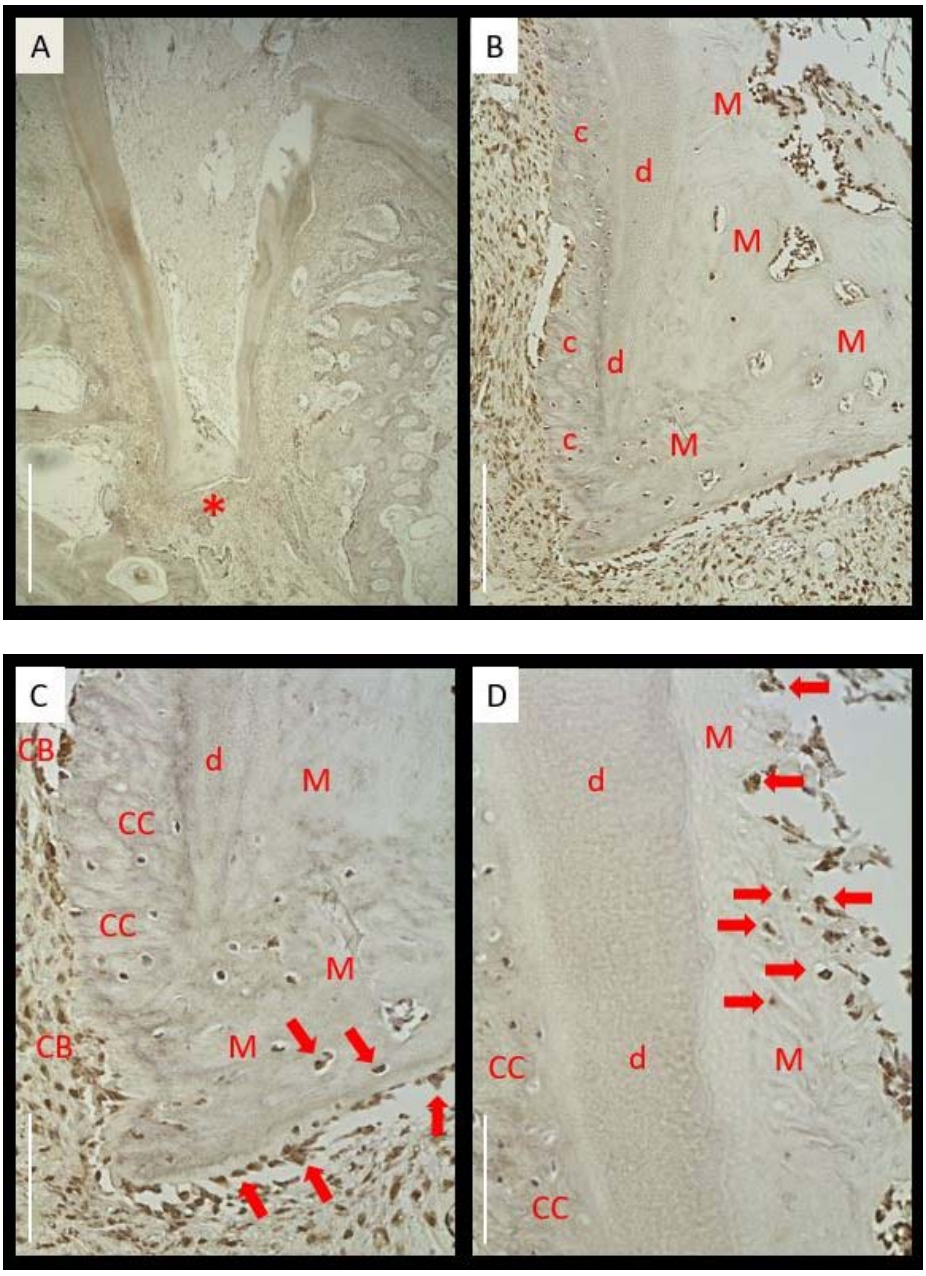

Figure 10: Group 2 **(A)** Representative sample a root and apex (star) of a biodentine and blood clot treated premolar stained with osterix marker (4x magnification, scale bar = 1 mm). **(B)** Mineralized matrix (M) lining internal surface of the canal wall, adjacent to dentin (d) and cementum (c). (20x magnification, scale bar = 200μm) **(C)** Layer of cells (arrows), strongly stained, overlaying the mineralized matrix (M) with strongly stained

embedded cells (arrows) within the matrix. Cementoblasts (CB), strongly stained, and cementocytes (CC), not stained, with osterix marker (lining the external surface of the root) (40x magnification, Scale bar =100μm). **(D)** At midroot, adjacent to dentin (d), mineralized matrix (M) with an adjacent layer of cells (arrows) and embedded cells (arrows), both strongly stained by osterix matrix. Cementocytes (CC) not stained. (40x Magnification, Scale bar =100μm).

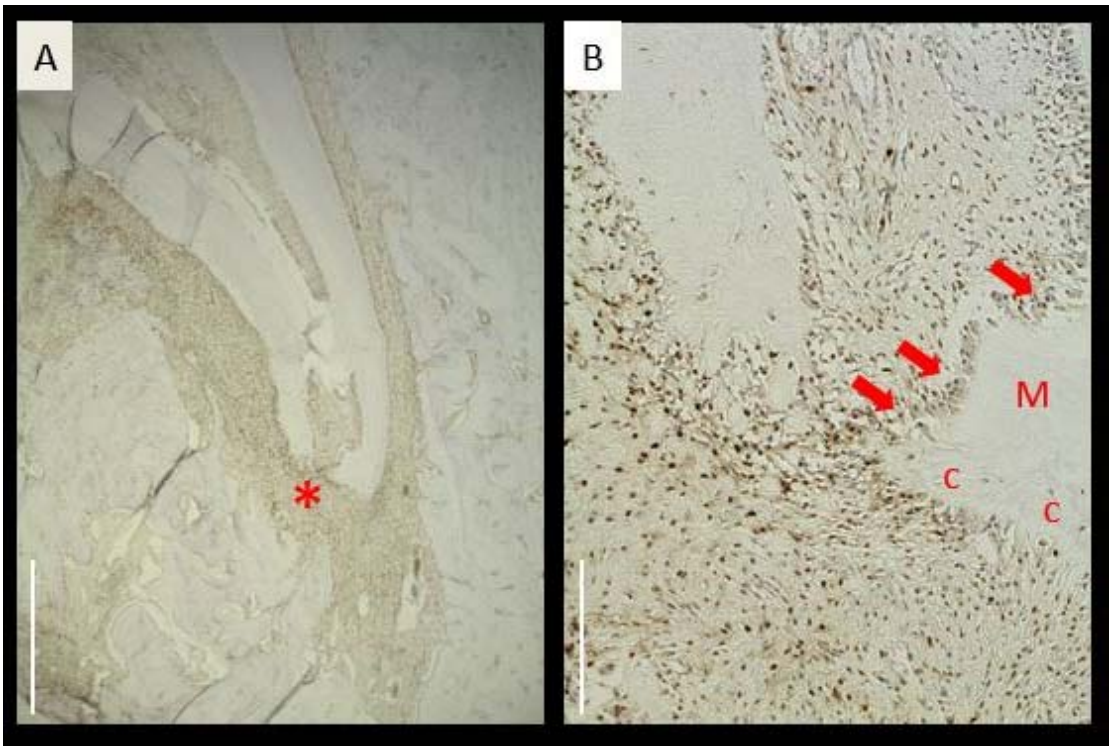

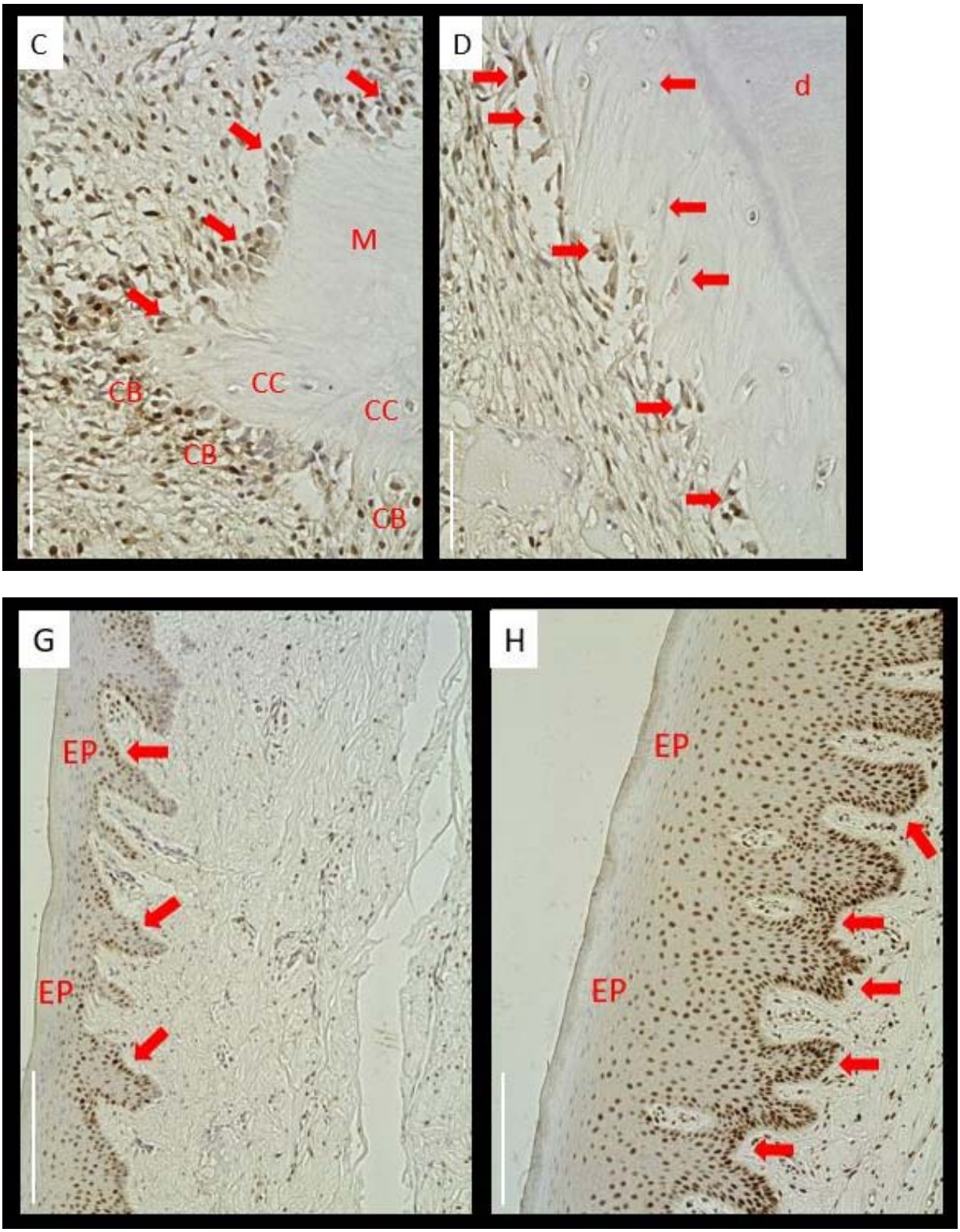

Figure 11: Group 3; **(A)** Representative sample of the root and apex (star) of a Biodentine and blood clot treated premolar stained with PCNA marker (4x magnification, scale bar = 1 mm). **(B)** At the apex, a layer of strongly stained cells (arrows) secreting a

mineralized matrix (M), lining the internal surface of the canal wall, adjacent to cementum (c) (20x magnification, scale bar = 200μm). **(C)** At the apex, layer of cells (arrows), strongly stained with PCNA marker, overlaying the mineralized matrix (M). Cementoblasts (CB), strongly stained, adjacent to cementum with cementocytes, not stained with PCNA marker (40x magnification, Scale bar =100μm). **(D)** At midroot, mineralized matrix (M) adjacent to dentin (d) and lining the internal wall of the call. A layer of cells (arrows), strongly stained, overlaying the mineralized matrix (M). Within the matrix, embedded cells (arrows) weakly stained by PCNA. (40x Magnification, Scale bar =100μm). **(E)** Bone of periodontium with strongly stained osteoblasts (OB) and weak and nonstained osteocytes (OC) marker (40x magnification, Scale bar =100μm). **(F)** Gingival papillae (P) with epithelium (EP) adjacent to tooth (4x magnification, scale bar = 1 mm). **(G)** Epithelium (EP) with strongly stained basal layer (arrows) (20x magnification, scale bar = 200μm). **(H)** Epithelium with strongly stained basal layer (arrows) with weakening of stain as epithelial cells migrate to external surface (40x Magnification, Scale bar =100μm).

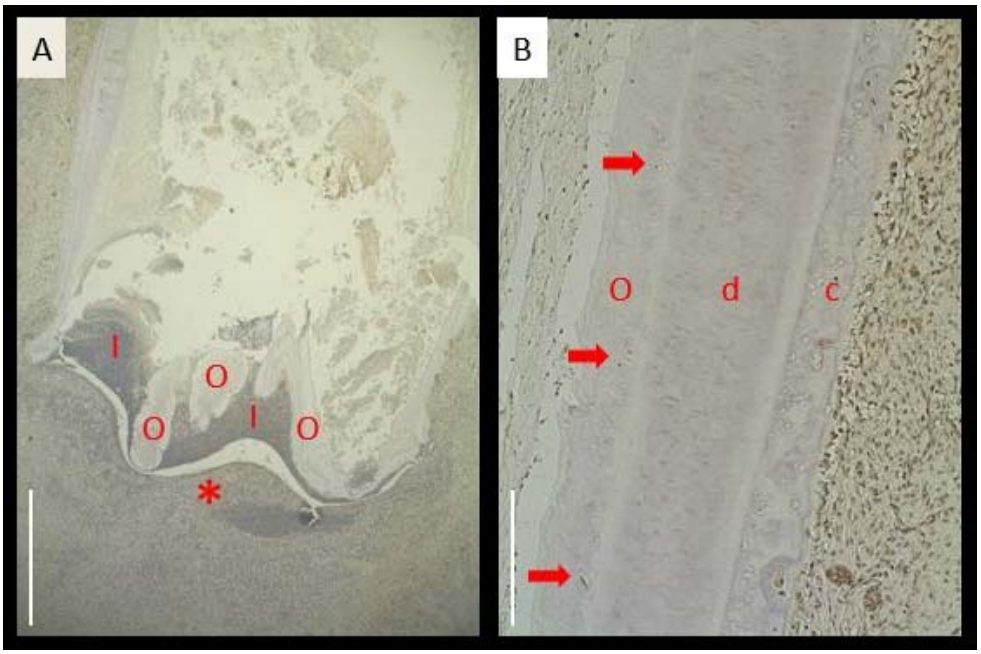

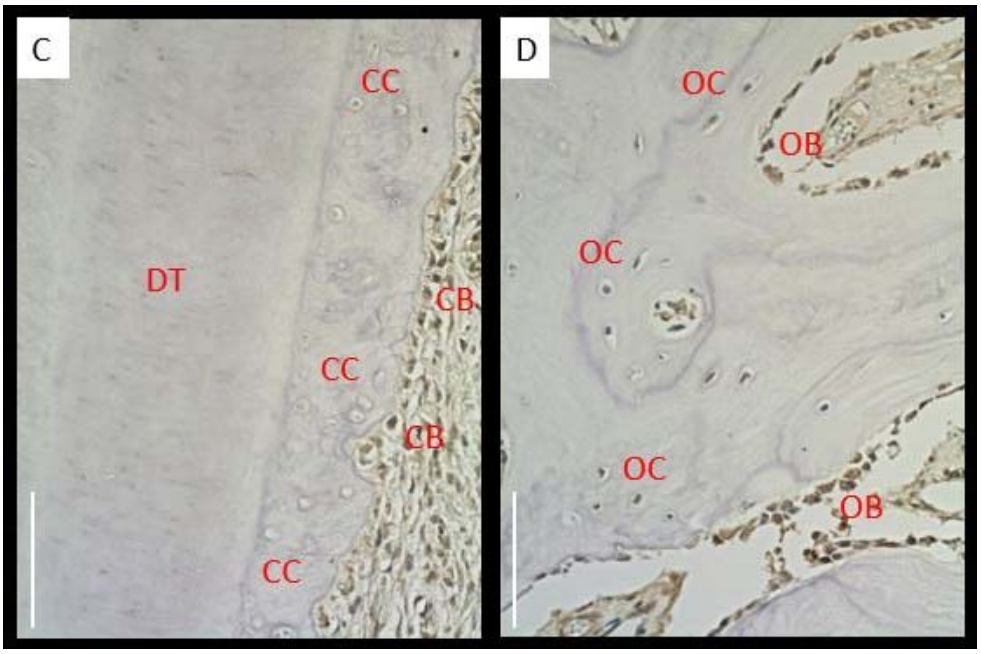

Figure 12: Group 3; **(A)** Representative sample of the root and apex (star) of a MTA and no blood clot treated premolar stained with CAP marker (4x magnification, scale bar = 1 mm). Moderate inflammatory infiltrate (I) surrounding osteoid-like matrix (O) **(B)** At midroot, adjacent to dentin (d) and cementum (c), osteoid-like mineralized matrix (O) with a few unstained embedded cells (arrows) (20x magnification, scale bar = 200μm) **(C)** At midroot, cementoblasts (CB), strongly stained, and cementocytes (CC), not stained, lining the external surface of the root. Dentinal tubules (DT) weakly stained by CAP (40x magnification, Scale bar =100μm). **(D)** Bone of the supporting periodontium with strong staining detected in osteoblasts (OB) and no staining detected in osteocytes (OC) (40x Magnification, Scale bar =100μm).

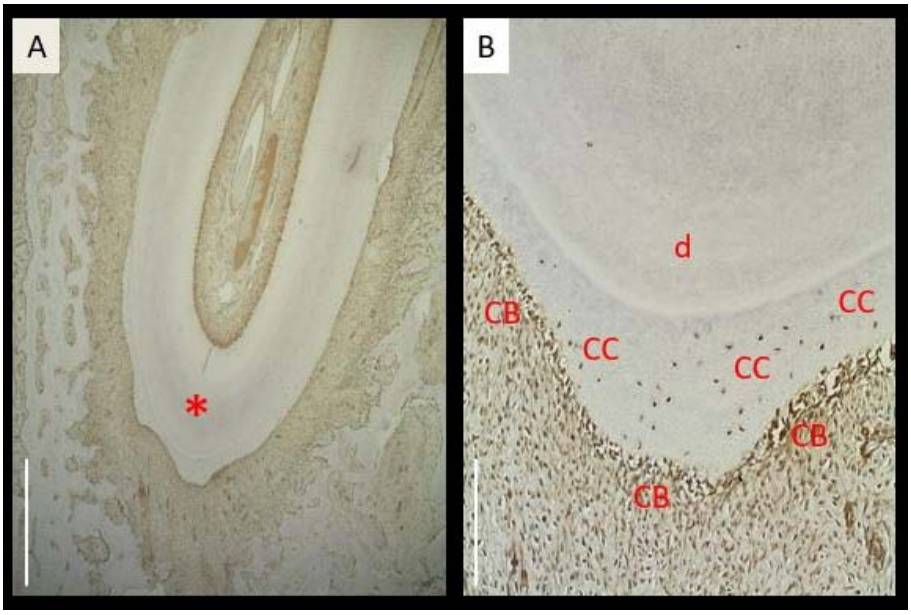

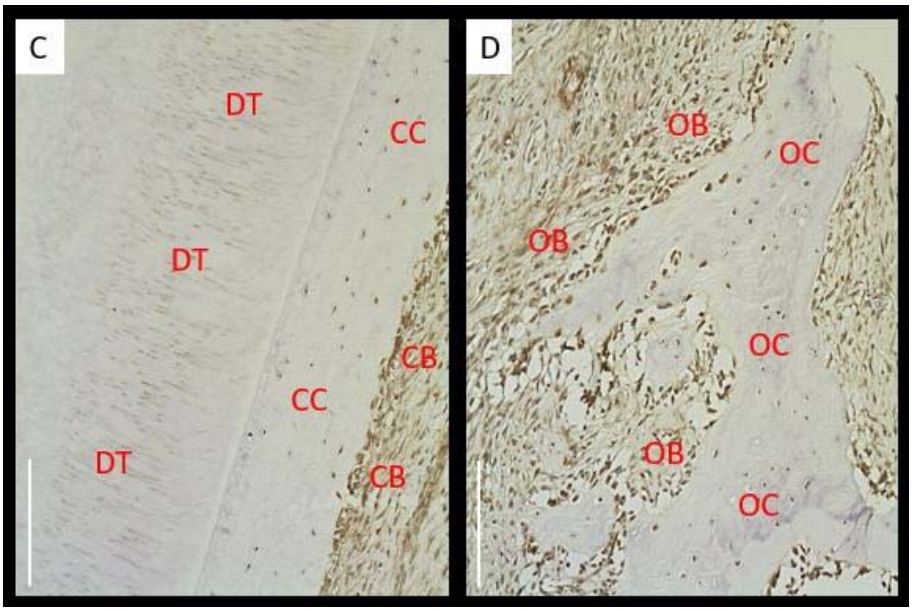

Figure 13: Group 3; **(A)** Representative sample of the root and apex (star) of a non-treated canine stained with CAP marker (4x magnification, scale bar = 1 mm). **(B)** At the apex, adjacent to dentin (d), lining the external surface of the root, cementoblasts (CB) stained strongly and cementocytes (CC) stained moderately with CAP (20x magnification, scale bar = 200μm) **(C)** At midroot, cementoblasts (CB) stained strongly and cementocytes (CC) stained moderately, and dentinal tubules (DT) stained weakly (20x magnification, Scale bar =200μm). **(D)** Bone of the supporting periodontium with strong staining detected in osteoblasts (OB) and weak staining detected in osteocytes (OC) (20x Magnification, Scale bar =200μm).